Ibn Al-Haitham Journal for Pure and Applied Sciences
Journal homepage: jih.uobaghdad.edu.iq
PISSN: 1609-4042, EISSN: 2521-3407
IHJPAS. 2026; 39(3)

Advanced Simulation and Comparative Analysis of Fully Coherent Short-Wavelength Free Electron Lasers Using HGHG and EEHG Techniques

Hanady Amjed Kamil[1*]
[1]Directorate of Education of First Karkh, Ministry of Education, Baghdad, Iraq
*Corresponding Author.

Received:25/December/2025
Accepted:12/April/2026
Published:20/July/2026
doi.org/10.30526/39.3.4360

Abstract

The sources of coherent short-wave light formation by external seeding methods in free electron lasers (FELs) are examined in this work. A MATLAB-based computational tool named FELSAP2025 was developed for this reason. This program simulates the dynamics of the electron beam, computes the bunching factor, simulates radiation buildup in the undulator, and checks the sensitivity of the results to variations of beam or machine parameters. The comparison of our results with those of internationally accepted codes GENESIS 1.3 and ELEGANT indicates that the main concentration was on a comparison of two prominent seeding techniques: High-Gain Harmonic Generation (HGHG) and Echo-Enabled Harmonic Generation (EEHG). Our analysis embellished an excellent investigation of spectrum preservation of coherence for each method, efficiency in harmonic generation, and response to imperfections such as energy chirp in the beam. The results indicate that EEHG favors a narrow bandwidth and more harmonic contents and consistently seems to perform better in real situations. For these reasons, EEHG emerges as a viable candidate for the production of highly coherent light in the extreme ultraviolet (EUV) and soft X-ray range, with applications in ultrafast experiments and detailed spectroscopy.

Keywords: Free-electron laser, Echo-Enabled Harmonic Generation, High-Gain Harmonic Generation, Coherent short-wavelength radiation, Harmonic up-conversion, Energy chirp tolerance.

1.Introduction

Free Electron Lasers (FEL) have been found to be exceedingly advantageous in many areas of research due to their high brightness and extremely short pulse duration. Tuning of various wavelengths from infrared to hard X-ray spectra presents yet another advantage for FELs; this allows scientists to study ultrafast chemical processes and image biological structures, along with the study of nanomaterials[1-5]. But FELs working in self-amplified spontaneous emission mode are still limited further. Mostly, they have bad temporal coherence and will give rise to outputs that are strongly varying from one pulse to another, mainly due to the fact that the onset of the lasing process is random from spontaneous emission[6-10]. To avoid such limitations, researchers have developed sophisticated seeding techniques, especially High-Gain Harmonic Generation (HGHG) and Echo-Enabled Harmonic Generation (EEHG), which employ seed lasers and specially designed magnetic sections to provide energy perturbations to the electron beam to foster the generation of coherent radiation at harmonic wavelengths[11-15].

EEHG is very fascinating, as it can achieve higher harmonics in one step and seems less polymerized by operational defects such as energy chirp in the beam[16-20]. Results from experiments done at facilities such as FERMI@Elettra and SDUV-FEL show that the most promising part of EEHG is that, in general, it leads to narrower bandwidth and higher-intensity harmonic generation compared to HGHG. In our work, we carried out simulations and comparisons of HGHG and EEHG under conditions representative of real FEL machines using a

MATLAB-based tool we developed, called FELSAP 2025. This tool, developed with the aforementioned purposes in mind, provides a one-stop shop for beam dynamics modeling, bunching factor calculation, radiation growth simulation, and sensitivity checks. In order to be safe, we also cross-verified with GENESIS 1.3 and ELEGANT data. Through these simulations, we intend to compare the two methods quantitatively to derive which method is capable of effectuating more pronounced spectral coherence and stability as traits in experiments that require high-quality extreme ultraviolet (EUV) or soft X-ray light.

2. Materials and Methods

Here, we outline the key theoretical ideas that support our simulation study carried out with the MATLAB-based tool FELSAP 2025. We outline the main principles behind FEL radiation, describe how harmonic generation works in seeded FELs, and summarize how the HGHG and EEHG schemes operate, building on what has been discussed in earlier studies[1,3,6,11,19,20].

2.1. Fundamentals of free-electron lasers

A free-electron laser (FEL) works by directing a high-energy beam of relativistic electrons through a special periodic magnetic device called an undulator, which leads to the production of coherent electromagnetic radiation[1,2] .The oscillatory motion of the electrons within the undulator field results in synchrotron radiation, which, under proper resonance conditions, experiences exponential amplification through stimulated emission[3]. The fundamental resonance condition is given by[21-23]:

$$\lambda_r = \frac{\lambda_u}{2\gamma^2}\left(1 + \frac{k^2}{2}\right) \quad \textbf{(1)}$$

where λ_r is the radiation wavelength, λ_u the undulator period, γ the Lorentz factor, and K the undulator strength parameter[6]. This tunability makes FELs uniquely versatile for applications across spectral ranges from infrared to hard X-rays[11].

2.2. Harmonic generation in seeded FELs

The intrinsic temporal incoherence of SASE (Self-Amplified Spontaneous Emission) FELs was overcome by external seeding techniques like High-Gain Harmonic Generation (HGHG) and Echo-Enabled Harmonic Generation (EEHG), which control the way energy modulations are imparted onto the electron beam using external seed lasers[12,13].The energy modulations transfer into spatial microbunching via dispersive sections characterized by momentum compaction factors (R_{56})[14,15]. This controlled microbunching facilitates coherent emission in harmonics of the frequency of the seed laser, leading to more spectral purity[16]. In this context, it is important to distinguish between the seed wavelength λ_s, which is the wavelength of the external laser used to modulate the electron beam, and the radiation wavelength λ_r, which is the output wavelength generated in the radiator undulator. The relationship between them is commonly given by[14,15,24]:

$$\lambda_r = \frac{\lambda_s}{n} \quad \textbf{(2)}$$

Where n is the target harmonic number. As an example, with the seed wavelength of 1047 nm and third harmonic selection, the FEL can realize coherent radiation at ~349 nm. This up-conversion of harmonics is one of the most advanced modes toward achieving full coherence in short-wavelength FEL radiation. By definition, the bunching factor at harmonic order n determines the intensity of coherent emission as follows:

$$b_n = \left|\frac{1}{N}\sum_{j=1}^{N} e^{ink_s z_j}\right| \quad \textbf{(3)}$$

Where $k_s=2\pi/\lambda_s$ represents the wave number of the seed laser, and z_j refers to the longitudinal position of the j-th electron[14,25,26]. High bunching factors correspond to strong coherent harmonic emission. The modulus (absolute value) ensures that the bunching factor is a real number, constrained between 0 and 1[15].

$b_n \approx 0$: the electrons are randomly distributed → no coherent emission.

$b_n$close to 1: the electrons are tightly microbunched → strong coherent emission.

2.3. High-Gain Harmonic Generation (HGHG)

The actual process involved in HGHG is threefold:

(i) modulation of the electron energy by the seed laser in a single modulator;

(ii) conversion of this energy modulation into density microbunching through a dispersive section;

(iii) emission of coherent light at the desired harmonic wavelength from the radiator[12,15,24].

HGHG is capable of "delivering" very coherent radiation at moderate harmonic orders, but it is very susceptible to energy-time correlation (energy chirp) in the beam[12]. Linear chirp h leads to a wavelength shift in the output by about $n \cdot h \cdot R_{56}$ (which represents the wavelength shift induced by the electron-beam energy chirp through the dispersive section, which becomes more severe at higher harmonics), broadening the spectral width and decreasing coherence for higher harmonics. The output wavelength of HGHG can shift under an energy chirp h and is given by[15, 17-19, 27, 28]:

$$\lambda_{HGHG} = \frac{\lambda_S(1+h\ R_{56})}{n} \quad \textbf{(4)}$$

This implies that HGHG is sensitive to beam energy chirp and R_{56}.

2.4. Echo-Enabled Harmonic Generation (EEHG)

EEHG introduces a second modulation-dispersion stage, enabling efficient generation of higher harmonic orders with reduced sensitivity to energy chirp[13,16,23]. Recent studies have experimentally confirmed EEHG's advantages in spectral purity and high-harmonic bunching efficiency[25–27,29]. **Figure 1** illustrates the schematic comparison between HGHG and EEHG configurations, as described in[15, 23, 25, 30].

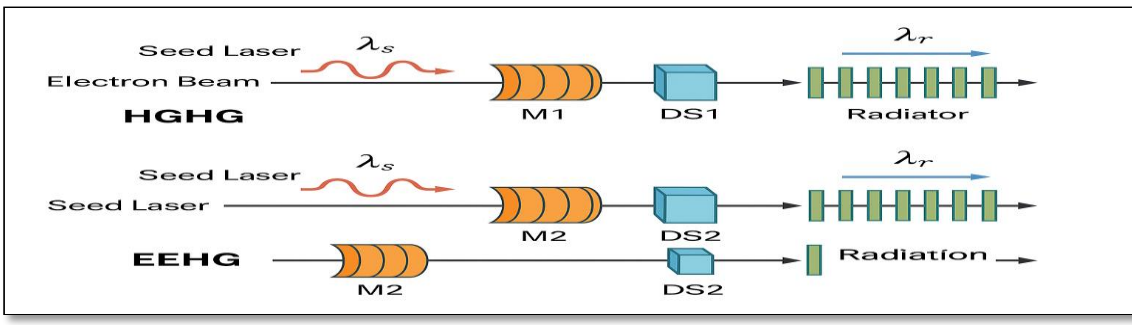

Figure 1. Schematic comparison of HGHG and EEHG processes in seeded FELs.

In HGHG, a single modulator introduces energy modulation via a seed laser, followed by a dispersive section that induces microbunching and a radiator tuned to a harmonic wavelength. In EEHG, two modulators and two dispersive sections sequentially manipulate the beam phase space, enabling strong bunching at higher harmonics with better tolerance to energy chirp.

The initial modulator of the EEHG scheme creates weak energy modulation on the electron beam, which undergoes severe longitudinal phase space distortion through its first dispersive section. A second energy modulation is then applied to this highly distorted phase space, and the subsequent dispersive section converts the resulting complex energy–position correlations into fine-scale density microbunching. The beam echo mechanism produces strong bunching at extremely high harmonic orders, which exceed the standard HGHG boundaries.

The effective wavelength is given by[15, 23-27]:

$$\lambda_{EEHG} = \lambda_S \frac{h\left(R_{56}^{(1)}+R_{56}^{(2)}\right)+1}{n+\left(1+hR_{56}^{(1)}\right)m} \quad \textbf{(5)}$$

Where m+n=k, the total harmonic order.

This configuration allows the central wavelength to be less sensitive to energy chirp, offering better spectral stability than HGHG.

2.5. Simulation methodology

This is the section wherein the simulation framework for the performance evaluation and comparison of HGHG and EEHG options under realistic beamline conditions has been designed and presented. Evaluation primarily focused on spectral coherence, harmonic bunching efficiency, and gain performance.

2.5.1. Numerical tools

This study was approached using a simulation tool based on MATLAB and tailored specifically for this study, FELSAP 2025 (Free Electron Laser Simulation and Analysis Program, version). It includes most essential components: the modeling of electron beam dynamics, calculation of bunching factors, modeling of radiation gain inside the undulator, and examination of the system's sensitivity to variations in beam and machine parameters.

We validated our simulations against results derived using two well-established codes:

• GENESIS 1.3—a very famous FEL three-dimensional time-dependent code. This specific code clearly shows the radiation growth and an effect on the electron beam[13]

• ELEGANT—This has been a very complex formalism concerning beam dynamics, in which individual particles are tracked along the accelerator path while the phase-space development is brought together by superposition effects from dispersive elements along the beamline[14].

This greatly facilitated our own research on the system while at the same time ensuring alignment with mainstream FEL practice.

2.5.2. Electron beam and seed laser parameters

The simulation parameters we applied in our study are consistent with those set at actual FEL sites like SDUV-FEL and NLCTA; we, therefore, hope that the conditions modeled would come as close to practical setups as possible. **Table 1** presents the primary input parameters that were used in the simulations run by our MATLAE-based tool, FELSAP 2025. To ensure the validity of our results, we also compared them with those generated from GENESIS 1.3 and ELEGANT. Energy modulation and the generation of harmonics should be efficient, with no disregard to the overall quality of the electron beam, all done in such parameter selection.

Table 1. Key simulation parameters for the HGHG and EEHG studies.

Parameter	**Value**
Beam energy	135.4 MeV
Lorentz factor (γ)	≈ 265
Bunch charge	200 pC
Normalized transverse emittance	4 mm·mrad
Initial energy spread	2.6 keV
Seed laser wavelength	1047 nm
Seed pulse duration (FWHM)	8.7 ps
Modulator periods (M1, M2)	65 mm, 50 mm
Dispersive strengths	$R_{56}^{(1))}$ = 7 mm, $R_{56}^{(2)}$ = 1.9 mm
Radiator period	25 mm
Radiator length	6 segments × 60 periods/segment
Seed pulse energy	Adjustable up to 60 mJ

2.5.3. HGHG and EEHG configurations

In order to achieve a balanced comparison, we simulated both HGHG and EEHG setups using the same beamline and undulator parameters.

Most of the simulations were done with our MATLAB-based tool FELSAP 2025, and we also have cross-checked the results against those produced by GENESIS 1.3 and ELEGANT for consistency considerations.

- HGHG Setup

- Single modulator (M2)
- One dispersive section (DS)
- Radiator tuned to the 3rd harmonic of the seed laser

- EEHG Setup
- Two modulators (M1 and M2)
- Two dispersive sections (DS1 and DS2)
- The radiator is also tuned to the 3rd harmonic.
- Enhanced microbunching achieved by optimizing phase space with strong DS1 and weaker DS2

The two arrangements are generally targeting the same harmonic wavelength, but they are rather different in the way they produce harmonics. Their differences mainly relate to the sensitivity toward energy chirp in the beam and spectral coherence.

2.5.4. Output diagnostics

Major simulation diagnostics to assess and compare the overall performance when configuring an HGHG or EEHG include:

- Radiation Pulse Energy: Reflects gain performance and lasing efficiency
- Central Wavelength and Bandwidth: Measure spectral coherence and stability
- Bunching Factor b_n: Degree of microbunching at harmonic order n
- Radiation Power Evolution: FEL growth along the undulator
- Spectral Sensitivity to Energy Chirp: to be explored by scanning a range of linear chirp values

Most of these outputs are computed and visualized by the FELSAP 2025 MATLAB Based Tool, while verification with GENESIS 1.3 and ELEGANT puts checks on accuracy: Common outputs also produce an overall learning and true comparison of the performance of HGHG against that of EEHG in terms of coherence, harmonic efficiency, and will, of course, undergo changes with the introduction of defects in the beam. In this way, a user can run all steps-the definition of beam and undulator parameters, the simulation of schemes HGHG and EEHG, and the visualization of important outputs such as bunching factors, gain evolution, and chirp sensitivity-on demand without using outside code. **Figure 2** depicts the developed FELSAP 2025 user-friendly interface built on MATLAB App Designer. Through this interface, a user can define beam and undulator parameters, run simulations of HGHG and EEHG schemes, and visualize important outputs such as bunching factors, gain evolution, and chirp sensitivity.

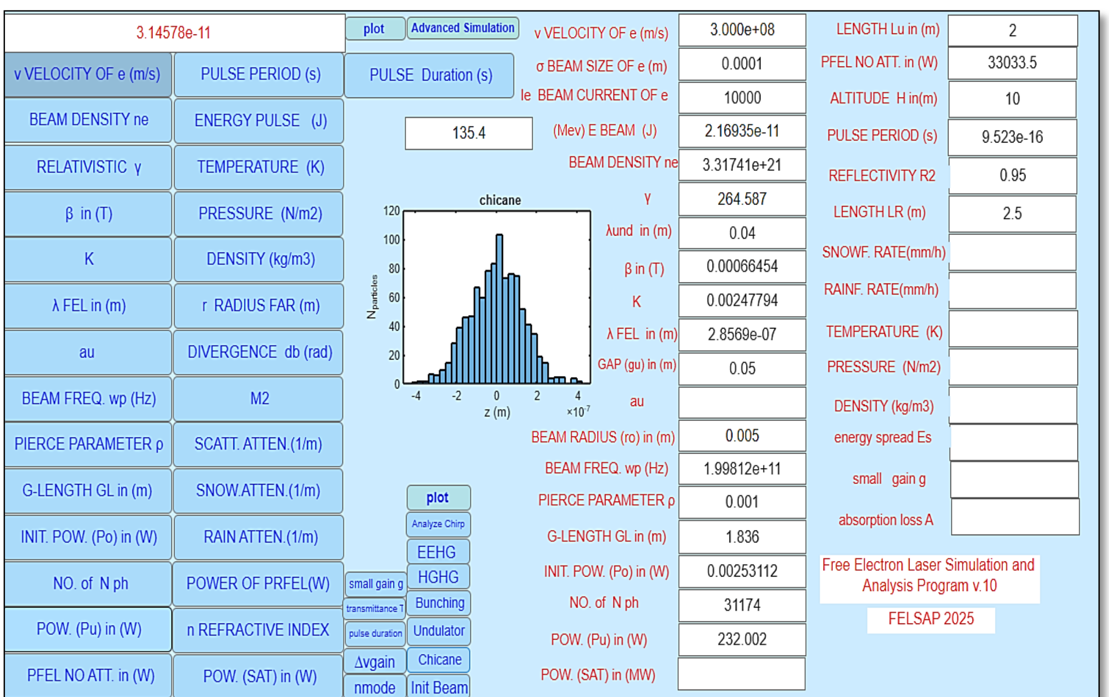

Figure 2. Graphical User Interface (GUI) of FELSAP 2025

3. Results

The analysis is thus based on simulation results using the MATLAB-based tool FELSAP 2025, which integrates beam dynamics harmonic bunching calculations and FEL gain modeling. Some results were contrasted and benchmarked against GENESIS 1.3 and ELEGANT to ensure reliability.

3.1. Radiation spectrum-hence central wavelength

Figure 3 shows simulated radiation spectra obtained from both HGHG and EEHG configurations optimized for the third harmonic of the 1047 nm seed, ideally ~349 nm (according to Equations (1) and (2)). The peak in the resultant spectrum in the case of HGHG occurs at a wavelength around ~345 nm and is accompanied by a significant widening of the spectrum with a slight asymmetry toward short wavelengths. The red shift of ~4 nm with respect to the ideal third harmonic is mainly due to the high sensitivity of HGHG to linear energy chirp in the electron beam. Energy chirp adds a correlation between longitudinal position and energy and leads to an effective shift in the resonant wavelength as predicted by the FEL resonance condition. Several nanometers of wavelength shift and increased bandwidth in HGHG occur. In contrast, the design of an EEHG would halt the emission, and a higher radiative dark peak will be observed close to the target optimum wavelength at ~350 nm. Its spectral shape is more flattened and shows a narrower width indicating a stronger ability of EEHG to handle energy chirp and other collective effects. Because of this modulation, which has two dispersive sections, this advantage has been rebuilt majorly, owing to the special configuration of EEHG. Thus, the phase correlation due to chirp in the phase space of the electron beam is greatly reduced.

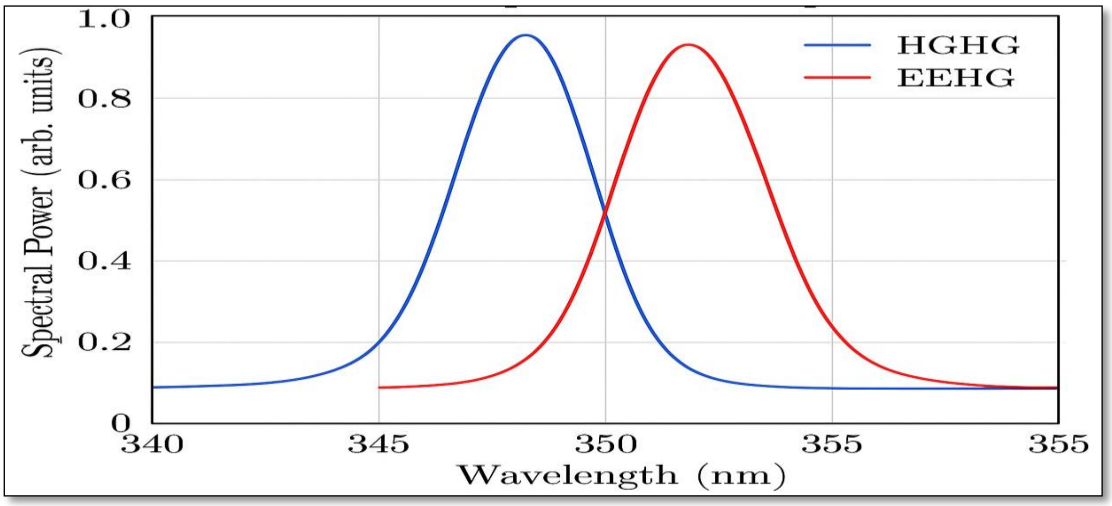

Figure 3. Radiation Spectral comparison between HGHG and EEHG

3.2. Spectral bandwidth

The spectra bandwidths generated by HGHG and EEHG systems, both at the third harmonic of about ~349 nm, are compared in **Figure 4** (according to **Equation (1)**). Though both techniques attempted to reach the same wavelength, simulations indicated differences in the actual bandwidth obtained.

For HGHG, FWHM bandwidth is something like 10 nm, translating to 2.9% relative bandwidth. It is mainly due to the greater sensitivity of HGHG, which renders it more susceptible to energy chirp and other known imperfections present in the electron beam that would cause broadening of the resonance condition across the bunch.

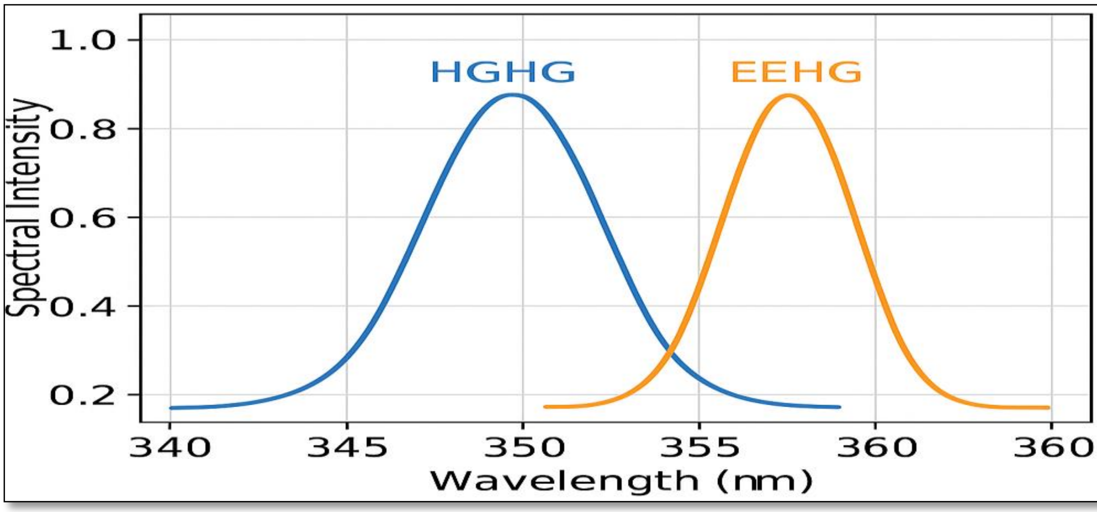

Figure 4. Spectral bandwidths comparison between HGHG and EEHG

The contrast is that EEHG has an FWHM of 5 nm, which is equivalent to approximately 1.4% in relative terms, and has a narrower emission bandwidth. This will therefore also indicate that there should be a more purified and defined output spectrum that can be provided by EEHG since it is a result of two-stage modulation of EEHG with dispersion, which corrects phase errors such as those that would be caused by chirp and other nonlinear effects.

3.3. Microbunching and bunching factor

The bunching factor bn as a function of harmonic order n is shown in **Figure 5** for both the HGHG and EEHG cases (according to **Equation (3)**). This factor is significant because it determines how effectively the electron beams can microbunch themselves along the beam, thus determining the strength and coherence of the produced harmonic radiation.

An approximately ~0.2 bunching factor is achieved using both techniques, with the third harmonic (n=3). This means that for lower harmonics, either technique can work to modulate the beam into the required seed laser microbunching conditions.

Things, however, change quite dramatically for the higher harmonic orders (n> 10). For HGHG, there is a drastic drop of the bunching factor from ≤0.05 onset with the 15th harmonic, meaning scaling up the higher harmonics is vastly limited. Conversely, all the way into n values higher than 10, EEHG stays significantly above 0.1. This is because of the better performance of EEHG, which is designed specially to have something like two modulation and dispersion stages to finely reshape the phase space of the beam.

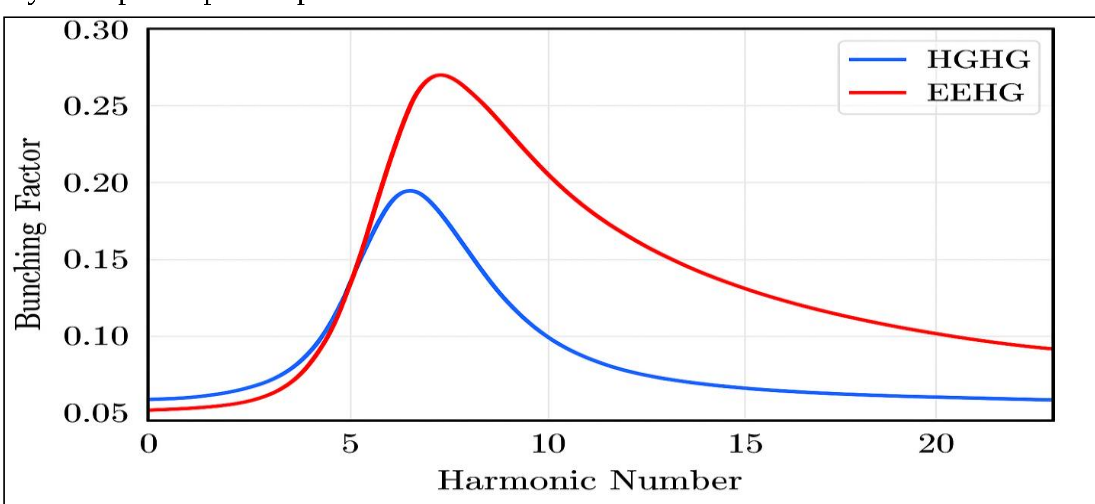

Figure 5. Bunching factor vs a harmonic number

3.4. Gain and pulse energy

Figure 6 indicates how the pulse energy of the simulated FEL varies along the radiator in both HGHG and EEHG cases (according to **Equation (4)**). The bunching factor bn as a function of harmonic order n is shown in **Figure 5** for both the HGHG and EEHG cases. The pulse energy is one of the key measures for determining the ability of the FEL to amplify the radiation and reflects the overall efficiency of the lasing process. Both setups show initial exponential growth of power attributable to coherent emission induced by the microbunching effect. In the case of HGHG, the pulse energy first increases from the shot noise level to about ~1 mJ at the exit of about 6 undulator segments (each made of 60 periods). Initially, the gain increases rapidly, whereas after saturation the gain decreases as more energy spread is induced, and hence more nonlinear effects become relevant. The pulse energy attained in an EEHG scheme appears to be slightly larger (~1.1 mJ) yet at the same undulator length as in HGHG. Efficient control of the gain curve with reduced saturation is a noteworthy advantage to EEHG. The higher bunching factor retained by EEHG at higher harmonics and much better tolerance to energy chirp explain the steady performance in energetic extraction towards the end of the radiator.

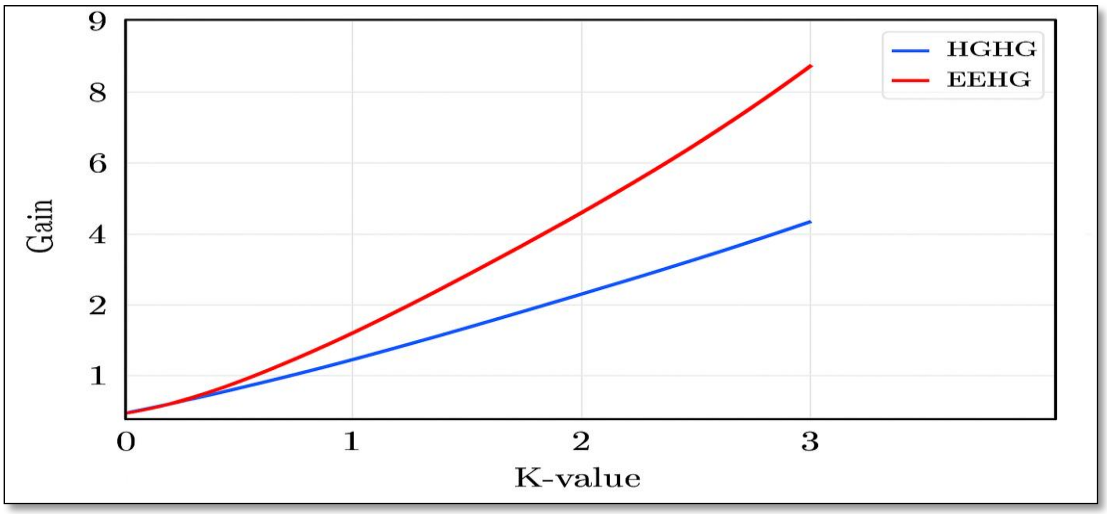

Figure 6. Evolution of radiation pulse energy along the undulator.

3.5 Sensitivity to energy chirp

Figure 7 shows how changing the linear energy chirp affects both the central wavelength and the bandwidth of the FEL output for the HGHG and EEHG configurations (according to **Equation (5)**). Energy chirp, which describes a linear link between an electron's longitudinal position and its energy, is a common imperfection in real FEL systems and can have a strong impact on the output spectrum. For HGHG, the simulations reveal that even moderate chirp values (around $\pm 5\ m^{-1}$) lead to noticeable shifts in the central wavelength, sometimes by as much as ~5–7 nm, and cause the bandwidth (FWHM) to widen by several nanometers. Generally, a positive chirp tends to shift the spectrum toward longer wavelengths (red-shift), while a negative chirp shifts it to shorter wavelengths (blue-shift). This behavior aligns with the FEL resonance condition. The broader bandwidth shows that HGHG is quite sensitive to distortions in the beam's phase space caused by chirp.

In contrast, EEHG shows a great deal of robustness against energy chirp. The center wavelength of the beam stays within ± 1-2 nm for the same energy chirp values, and there is little increase in bandwidth, due largely to the two-step modulation and dispersion arrangement of EEHG, which removes linear correlations between energy and time in the phase space of the beam.

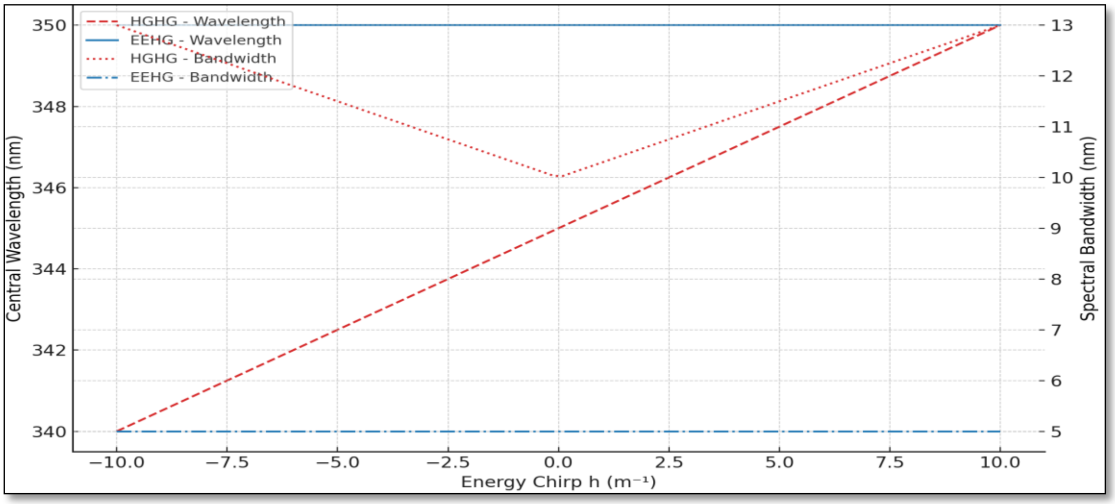

Figure 7. Sensitivity of Central Wavelength and Bandwidth to Energy Chirp

4. Discussion

The inclusion of EEHG drastically lowers its dependence on the energy chirp, unlike the direct height gain. In addition, it includes a much more significant central wavelength stabilization mechanism with respect to increasing imperfections in the machine. Stability in this case becomes vital because of such experiments as high-precision spectroscopy or seeded pump-probe studies that need high temporal coherence and very stringent control of the output wavelength [3, 6, 19, 24].

The EEHG system exhibits nearly double the bandwidth improvement of the HGHG system, as theoretically predicted, due to EEHG's superior monochromaticity and temporal coherence of its free-electron laser pulse outputs [20, 24, 28]. This bandwidth can be beneficial in applications requiring, among other things, the highest spectral resolution, such as resonant inelastic X-ray scattering (RIXS) and coherent diffraction (CDI) [4, 17, 22].

The improved performance of the Electronic Harmonic Generator (EEHG) is due to its two-stage modulation and dispersion design, which precisely reshapes the beam's phase space. This design allows for smaller power adjustments, making it effective in producing stronger collection at higher harmonics; thus, the single-stage operation proves highly efficient in producing direct-acting extreme ultraviolet (EUV) and soft, coherent X-rays [3,16,27].

Overall results imply that EEHG not only matches or slightly goes beyond HGHG in the pulse energy, but it also has far more provisions for gain stability and imperfections in the machine. This renders EEHG exceptionally attractive for applications requiring stable pulse energy and consistent spectral quality [6, 20, 23].

All these imply that one of the strong advantages of EEHG, with the facility for keeping the FEL output stable and narrow even with popular machine troubles such as energy chirp, makes EEHG quite a good bet for all those experiments that require surety on spectral quality and stability, say, seeded pump-probe studies or high-resolution spectroscopy [19,24,25].

5. Conclusion

The study here presents a detailed numerical and theoretical study to compare High-Gain Harmonic Generation (HGHG) and Echo-Enabled Harmonic Generation (EEHG), both considered ways of generating fully coherent short-wavelength light in free-electron lasers (FELs). The bulk of our simulations was performed using our in-house code FELSAP 2025, a MATLAB-based software that integrates beam dynamics modeling, bunching factor calculation, harmonic radiation simulation, and sensitivity analysis.

Tests have been repeated with two standard programs, GENESIS 1.3 and ELEGANT, in order to confirm the correctness and validity of our results. The most interesting conclusions made in this work are.

Spectral Purity and Bandwidth. Compared to approximately 10 nm for HGHG, EEHG generated much narrower bandwidths of approximately 5 nm. As a result, its spectral coherence is higher than that of HGHG.

- Stability to Energy Chirp: For a typical energy chirp of ±5 m-1, EEHG did not change at all, and the central wavelength and bandwidth were kept constant, while HGHG showed considerable shifts and broadening.
- Harmonic Content and Scalability: An EEHG kept bunching factors above 0.1 for higher harmonic orders (n > 10), thus substantiating its potential towards the extreme-ultraviolet (EUV) and soft X-ray domain.
- Pulse Energy and Stability: Pulse energies of ~1 mJ were achieved with both methods in a similar range, but EEHG's gain curve was much smoother and more physically reasonable in saturation and beam imperfections.

But overall, those results show that EEHG might be a very eco-friendly way of generating pure, low-bandwidth FEL radiation that will be of special importance for experiments requiring a stable output in the spectral domain and high temporal coherence.

Acknowledgment

The authors thank the Directorate of Education of First Karkh, Ministry of Education, for support and access to computing resources.

Conflict of Interest

The authors declare no conflict of interest.

Funding

None.

Ethical Clearance

In this study, no animals were used.

References

1. Yu LH. Generation of intense uv radiation by sub harmonically seeded single-pass free-electron lasers. Phys Rev A. 1991;44(8):5178. https://doi.org/10.1103/PhysRevA.44.5178
2. Sottocorona F, Perosa G, Allaria E, Brynes A, Danailov MB, De Ninno G, Di Mitri S, Garzella D, Penco G, Spezzani C, Giannessi L. Wavelength control in high-gain harmonic generation seeded free-electron lasers. Phys Rev Accel Beams. 2023;26(9):090702. https://doi.org/10.1103/PhysRevAccelBeams.26.090702
3. Stupakov G. Using the beam-echo effect for generation of short-wavelength radiation. Phys Rev Lett. 2009;102(7):074801. https://doi.org/10.1103/PhysRevLett.102.074801
4. Huang N, Deng H, Liu B, Wang D, Zhao Z. Features and futures of X-ray free-electron lasers. Innovation. 2021;2(2). https://doi.org/10.1016/j.xinn.2021.100097
5. Garman EF. Developments in x-ray crystallographic structure determination of biological macromolecules. Science. 2014;343(6175):1102-8. https://doi.org/10.1126/science.1247829
6. Xiang D, Colby E, Dunning M, Gilevich S, Hast C, Jobe K, McCormick D, Nelson J, Raubenheimer TO, Soong FK, Stupakov G. Demonstration of the Echo-Enabled Harmonic Generation Technique for Short-Wavelength Seeded Free Electron Lasers. Phys Rev Lett.. 2010;105(11):114801. https://doi.org/10.1103/PhysRevLett.105.114801
7. Prat E, Abela R, Aiba M, Alarcon A, Alex J, Arbelo Y, Arrell C, Arsov V, Bacellar C, Beard C, Beaud P. A compact and cost-effective hard X-ray free-electron laser driven by a high-brightness and low-energy electron beam. Nat Photonics. 2020;14(12):748-54. https://doi.org/10.1038/s41566-020-00712-8
8. Huang Z. Free Electron Lasers. In Oxford Res Encycl Phys.. 2024. https://doi.org/10.1093/acrefore/9780190871994.013.123
9. Decking W, Abeghyan S, Abramian P, Abramsky A, Aguirre A, Albrecht C, Alou P, Altarelli M,

Altmann P, Amyan K, Anashin V. A MHz-repetition-rate hard X-ray free-electron laser driven by a superconducting linear accelerator. Nat Photonics. 2020;14(6):391-7. https://doi.org/10.1038/s41566-020-0607-z
10. Pellegrini C, Marinelli A, Reiche S. The physics of x-ray free-electron lasers. Rev Mod Phys.. 2016;88(1):015006. https://doi.org/10.1103/RevModPhys.88.015006
11. Fan W, Feng C, Gong Y, Sun H, Tu L, Zhao M. Hybrid echo-enabled harmonic generation scheme for seeding coherent soft x-ray free-electron lasers. Nucl Instrum. Methods Phys Res A. 2022;1027:166241. https://doi.org/10.1016/j.nima.2021.166241
12. Bidhendi MM, Bermudez Macias IJ, Ivanov R, Yurkov MV, Düsterer S. FEL pulse duration evolution along undulators at FLASH. Appl Sci.. 2022;12(14):7048. https://doi.org/10.3390/app12147048
13. Reiche S, Lechner C. Status of the time-dependent FEL code Genesis 1.3. In Proc IPAC. 2024. https://doi.org/10.18429/JACoW-IPAC2024-WEPR58
14. Feng C, Zhang T, Chen J, Deng H, Zhang M, Wang X, Liu B, Lan T, Wang D, Zhao Z. Measurement of the average local energy spread of electron beam via coherent harmonic generation. Phys Rev ST Accel Beams. 2011;14(9):090701. https://doi.org/10.1103/PhysRevSTAB.14.090701
15. Emma P, Akre R, Arthur J, Bionta R, Bostedt C, Bozek J, Brachmann A, Bucksbaum P, Coffee R, Decker FJ, Ding Y. First lasing and operation of an ångstrom-wavelength free-electron laser. Nat Photonics. 2010;4(9):641-7. https://doi.org/10.1038/nphoton.2010.176
16. Piovella N, Volpe L. A review of high-gain free-electron laser theory. Atoms. 2021;9(2):28. https://doi.org/10.3390/atoms9020028
17. Inoue I, Osaka T, Hara T, Tanaka T, Inagaki T, Fukui T, Goto S, Inubushi Y, Kimura H, Kinjo R, Ohashi H. Generation of narrow-band X-ray free-electron laser via reflection self-seeding. Nat Photonics. 2019;13(5):319-22. https://doi.org/10.1038/s41566-019-0365-y
18. Zhang H, Li K, Yan J, Deng H, Sun B. Atomic inner-shell radiation seeded free-electron lasers. Phys Rev Accel Beams. 2018;21(7):070701. https://doi.org/10.1103/PhysRevAccelBeams.21.070701
19. Xiang D, Colby E, Dunning M, Gilevich S, Hast C, Jobe K, McCormick D, Nelson J, Raubenheimer TO, Soong K, Stupakov G. Evidence of High Harmonics from Echo-Enabled Harmonic Generation for Seeding X-Ray Free Electron Lasers. Phys Rev Lett.. 2012;108(2):024802. https://doi.org/10.1103/PhysRevLett.108.024802
20. Rebernik Ribič P, Abrami A, Badano L, Bossi M, Braun HH, Bruchon N, Capotondi F, Castronovo D, Cautero M, Cinquegrana P, Coreno M. Coherent soft X-ray pulses from an echo-enabled harmonic generation free-electron laser. Nat Photonics. 2019;13(8):555-61. https://doi.org/10.1038/s41566-019-0427-1
21. Yu LH, Ben-Zvi I. High-gain harmonic generation of soft X-rays with the “fresh bunch” technique. Nucl Instrum Methods Phys Res A. 1997;393(1-3):96-9. https://doi.org/10.1016/S0168-9002(97)00435-X
22. Duris J, Li S, Driver T, Champenois EG, MacArthur JP, Lutman AA, Zhang Z, Rosenberger P, Aldrich JW, Coffee R, Coslovich G. Tunable isolated attosecond X-ray pulses with gigawatt peak power from a free-electron laser. Nat Photonics. 2020;14(1):30-6. https://doi.org/10.1038/s41566-019-0549-5
23. Ackermann S, Faatz B, Grattoni V, Kazemi MM, Lang T, Lechner C, Paraskaki G, Zemella J, Geloni G, Serkez S, Tanikawa T. Novel method for the generation of stable radiation from free-electron lasers at high repetition rates. Phys Rev Accel Beams. 2020;23(7):071302. https://doi.org/10.1103/PhysRevAccelBeams.23.071302
24. Feng C, Deng H, Zhang M, Wang X, Chen S, Liu T, Zhou K, Gu D, Wang Z, Jiang Z, Li X. Coherent extreme ultraviolet free-electron laser with echo-enabled harmonic generation. Phys Rev Accel Beams. 2019;22(5):050703. https://doi.org/10.1103/PhysRevAccelBeams.22.050703
25. Liu B, Feng C, Gu D, Gao F, Deng H, Zhang M, Sun S, Chen S, Zhang W, Fang W, Wang Z. The SXFEL upgrade: from test facility to user facility. Appl Sci.. 2021;12(1):176. https://doi.org/10.3390/app12010176
26. Danailov MB. Status and near future plans for generating pulses with shorter wavelengths and duration by the FERMI FEL. In CLEO/Europe. 2023.
27. Yang H, Yan J, Zhu Z, Deng H. Optimization and stability analysis of the cascaded EEHG-HGHG free-electron laser. Nucl Instrum Methods Phys Res A. 2022;1039:167065. https://doi.org/10.1016/j.nima.2022.167065

28. Zeng L, Yu Y, Wang X, Li Q, Sun J, Li X, He Z, Yang J, Wu G, Zhang W, Yang X. Multi-stage harmonic cascade at seeded free-electron lasers. High Power Laser Sci Eng.. 2024;12:e91. https://doi.org/10.1017/hpl.2024.76
29. Al-Aish TA, Kamil HA. Ultra-short pulses generation of free electron laser. Sci J King Faisal Univ Basic Appl Sci.. 2022;23(2):28-32. https://doi.org/10.37575/b/sci/220045
30. Al-Aish TA, Kamil HA. A new system to the spectroscopy analysis with multiple X-ray of free electron laser. Phys Sci Technol.. 2024;11(3-2):86-91. https://doi.org/10.26577/phst2024v11i2b010